

Superconductivity of Sn-Zn Eutectic Alloys

O. S. LUTES AND D. A. CLAYTON

Honeywell Research Center, Hopkins, Minnesota

(Received 2 December 1965)

An experimental study has been made of the superconducting transitions in Sn-Zn eutectic alloys in the temperature range 3.0–3.7°K, employing magnetization measurements on spherical samples. The samples were about 4 mm in diameter, and the laminar spacing varied from 1 to 8 μ depending on the speed with which the parent ingot had been cooled from the melt. The measurements showed magnetic isotherms approaching those of a type-I superconductor, but with frozen flux of varying degree. The critical-field-versus-temperature relation was similar to that of pure Sn, providing evidence that the laminations behave like a continuous superconducting material. The transition temperature T_c was found to decrease with decreasing laminar spacing. This effect was compared quantitatively with the predictions of proximity-effect theory. The two significant theoretical parameters derived from the data were ρ_s , the effective resistivity ratio of the Sn-rich phase, and T_{cn} , the effective transition temperature of the Zn-rich phase. The large-spacing T_c data indicated an effective ρ_s of about 0.12, in reasonable agreement with the expected magnitude. At smaller spacing the experimental T_c was higher than expected. Alternatively stated, T_{cn} was 2.7°K, which is larger than the accepted Zn transition temperature 0.9°K.

INTRODUCTION

A LARGE amount of experimental work, beginning with that of Meissner,¹ has demonstrated the existence of a “proximity effect” at the contact between a normal and a superconducting metal. The most frequently studied type of system has been that of superimposed thin films deposited from the vapor.² An important concept developed from the film studies was that in a superimposed system of sufficiently thin layers the superconductivity is that of the system as a whole, i.e., the normal layer becomes superconducting because of its proximity to the adjacent superconducting material. The transition temperature of such a system will be lower than that of the isolated superconductive member by an amount depending on the purity and thickness of the two films.

Proximity effects should also be observable in systems other than superimposed films, provided such systems in some way consist of small-dimensioned superconducting regions in contact with normal regions. A recent investigation of Cu-Pb alloys has indicated superconductive transitions occurring at temperatures which depend on the dimensions of the Pb inclusions.³ Another type of structure which should meet the requirements is a eutectic alloy consisting of alternating laminations of superconducting and normal metal. The Pb-Sn eutectic system has already been investigated by Shiffman, *et al.*,⁴ using specific-heat measurements. These measurements, which were made on one laminar spacing, showed an alteration in the specific-heat jump near the Sn

transition, relative to that calculated on the basis of additivity, and the results were attributed to proximity effects. The present investigation consists of magnetic measurements on the Sn-Zn eutectic system in the temperature range from 3.0 to 3.7°K. The object was a comparison of the superconducting behavior of such systems with the predictions of proximity effect theory, with particular attention given to the influence of the laminar spacing of the alloy. The results⁵ show some disagreement with the theory, but, in general, the shape of the magnetic isotherms, the form of the critical-field curve, and the monotonic decrease of transition temperature with decreasing laminar spacing, are in accordance with the expected proximity effects.

EXPERIMENTAL PROCEDURE

Sample Preparation

The samples were prepared from Cominco 69-grade Sn and Zn pellets and were weighed out in the proportions of 91% Sn and 9% Zn, corresponding to the eutectic concentration.⁶ The pellets were placed together in a sealed, evacuated, 8-mm diam Pyrex tube. The charge was melted and allowed to solidify. After examination the ingot was cast into a smaller tube, 4 mm in diameter, which could be suspended in a furnace. The tube was lowered out of the furnace at a rate varying with sample between 0.3 and 8.8 cm/h. This procedure resulted in the well-known laminar structure⁷ in which the laminar planes are parallel to the direction of temperature gradient, in this case the axis of the specimen, and for which the laminar period depends inversely on the growth rate. Laminar spacings varied

¹ H. Meissner, Phys. Rev. **109**, 686 (1958); **117**, 672 (1960).

² P. H. Smith, S. Shapiro, J. L. Miles, and J. Nicol, Phys. Rev. Letters **6**, 686 (1961). P. Hilsch, Z. Physik **167**, 511 (1962). W. A. Simmons and D. H. Douglass, Jr., Phys. Rev. Letters **9**, 153 (1962). J. J. Hauser, H. C. Theurer, and N. R. Werthamer, Phys. Rev. **136**, A637 (1964). J. J. Hauser and H. C. Theurer, Phys. Rev. Letters **14**, 270 (1965).

³ C. J. Raub and E. Raub, Z. Physik **186**, 310 (1965).

⁴ C. A. Shiffman, J. F. Cochran, M. Garber, and W. Pearsall, Rev. Mod. Phys. **36**, 127 (1964).

⁵ A preliminary account of the results was presented previously. See O. S. Lutes and D. A. Clayton, Bull. Am. Phys. Soc. **10**, 347 (1965).

⁶ Max Hansen, *Constitution of Binary Alloys* (McGraw-Hill Book Company, Inc., New York, 1958), 2nd ed., p. 1218.

⁷ W. C. Winegard, S. Majka, B. M. Thall, and B. Chalmers, Can. J. Chem. **29**, 320 (1951).

from 0.8 to 7.5 μ . Figure 1 shows photomicrographs taken of slices made perpendicular to the axis of each ingot. Boundaries may be observed between regions having different laminar orientations, but the measured lamellar period is about the same for all regions of a section, indicating that the planes are parallel to the axis as expected, the orientations of the different regions differing only by rotations about this axis.

The samples which were used in the subsequent magnetic measurements were spheres measuring about 0.38 cm in diameter. The spheres were made from the cylindrical ingot rods in the following way. One end of the cylinder was cemented in a brass holder which could be rotated by a motor. The free end of the cylinder was first shaped roughly by beveling the end with a file. The end was then lapped by rotation in a hemispherical cavity in a stainless steel plate, using Al_2O_3 lapping compound. The protruding end of the cylinder was cut off slightly longer than the desired diameter and the hemispherical end cemented in place in a matching hole in a second holder. The opposite end was then lapped into hemispherical shape by the same process. The resulting sphere varied in diameter by less than 2% over the surface. Microscopic examination of a sectioned portion of a sphere revealed superficial irregularities extending a few microns in depth. A corresponding depth was etched off the sample spheres using a mixture of CrO_3 , Na_2SO_4 , and H_2O . Volumes were determined from micrometer determinations of the average diam-

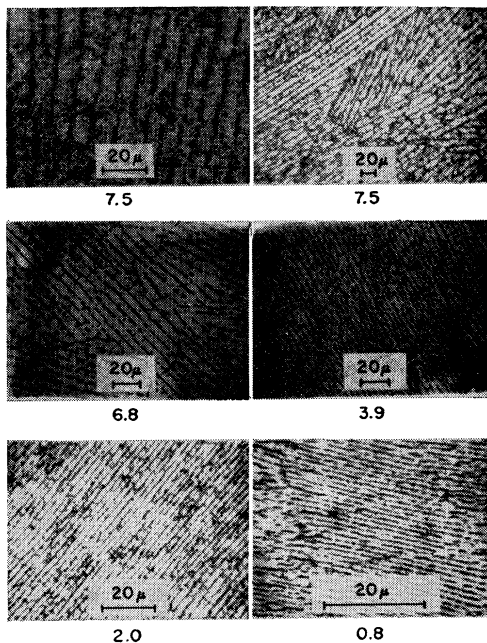


FIG. 1. Photomicrographs of lamellar structure. Surfaces are planes lying perpendicular to direction of temperature gradient in the various ingots. Ingots are identified by period in microns given below each photograph. Scale is given by length of 20- μ symbol on photograph. Eutectic domains may best be seen in photomicrograph on upper right.

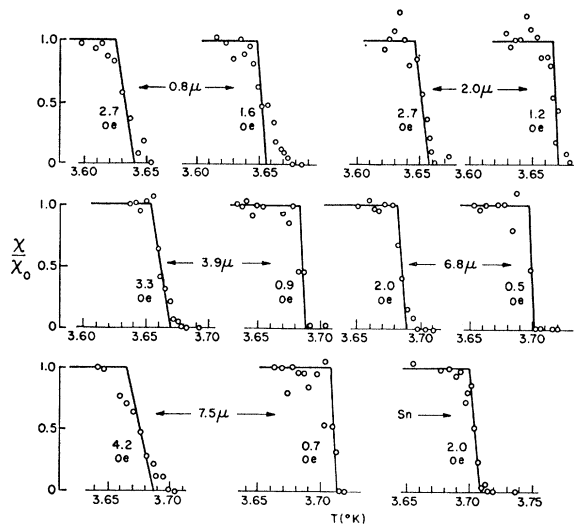


FIG. 2. Constant-field transitions near T_c . Abscissa gives temperature. Ordinate shows ratio of magnetic moment of sample to that in superconducting state. Solid curves give expected transitions for type-I superconductors calculated for the applied fields indicated.

eters. The spheres were annealed for a total time of two weeks at 140°C. They were mounted for magnetic measurements with the lamellar planes parallel to the magnetic field.

Measurement Technique

The dependent variable in these measurements was the magnetic moment of the sample sphere, while the independent variables were temperature and applied magnetic field. The magnetic moment was measured by a sample displacement technique previously described.⁸ During measurements the sample was immersed in liquid helium. Vapor-pressure thermometry and temperature control were accomplished by standard techniques. An auxiliary carbon resistance thermometer was mounted near the sample to monitor any local temperature changes. The magnetic field was furnished by a 12-in. Varian magnet in which the power supply had been adapted for small field (<100 Oe) measurements by shunting the controlled current. Measurements of field were made with a rotating-coil gaussmeter. Absolute calibration of both the gaussmeter and the magnetic-moment apparatus was based on magnetic-isotherm determinations on a pure Sn sphere, assuming a critical-field-versus-temperature relationship appearing in the literature,⁹ and the theoretical magnetic susceptibility $-(3/8\pi)$ of a superconducting sphere.

Determination of Transition Temperatures and Critical Fields

The transition temperature T_c was determined by extrapolating the critical field H_c to zero, using experi-

⁸ O. S. Lutes and J. L. Schmit, Phys. Rev. **125**, 433 (1962); **134**, A676 (1964).

⁹ E. Maxwell and O. S. Lutes, Phys. Rev. **95**, 333 (1954).

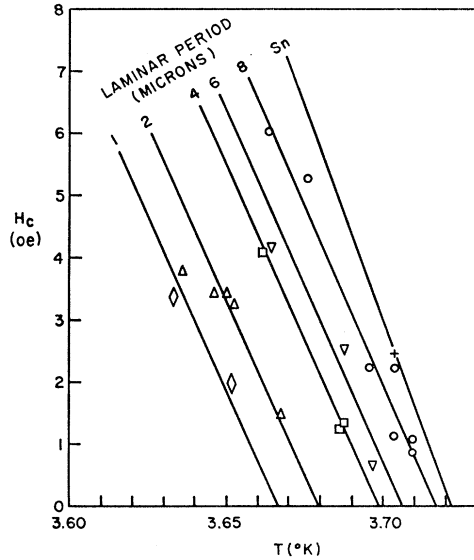


FIG. 3. H_c versus T near T_c . Experimental data are shown together with straight lines having the approximate average slope of all the samples. For the pure-Sn slope the line was drawn to have a slope of $140 \text{ Oe } (^{\circ}\text{K})^{-1}$.

mental H_c values near T_c . H_c was determined by measuring the magnetic moment of the sample in a constant field of a few oersteds as the temperature was increased incrementally. The temperature changes were monitored by the vapor pressure of the bath, as well as by the resistance thermometer attached near the sample. The resistance thermometer was found to follow the vapor-pressure changes closely, indicating that the heat leak into the bath was adequate to bring about equilibrium. The small fields applied to the sample were brought about by demagnetization of the magnet pole pieces to the proper level. The remanent field could be nulled to within a few hundredths of an oersted by applying current to the magnet windings from an external source.

In addition to the measurements near T_c , magnetic-isotherm measurements were carried out at a lower temperature 3.277°K in order to compare the critical fields and isotherm shapes of the different samples with each other and with pure Sn.

RESULTS AND DISCUSSION

Results for H_c and T_c

Characteristic transitions near T_c at constant field are shown in Fig. 2 for all samples. The form of such transitions is readily derivable for a type-I superconducting sphere on the assumptions of (a) perfect diamagnetism at temperatures less than that of the transition, (b) uniform magnetization throughout the sphere, and (c) the field at the equator has its critical value at any temperature in the transition region. This leads to the following relations for the magnetization M

and transition breadth $(\Delta T)_{21}$:

$$M/M_1 = 1 - (2/H)(T - T_1)|dH_c/dT|, \quad (1)$$

$$(\Delta T)_{21} = H/2|dH_c/dT|, \quad (2)$$

where the subscripts 1 and 2 refer to the temperatures at which the field begins and completes its penetration, respectively, H is the magnitude of the applied field, and dH_c/dT is the slope of the critical field-versus-temperature curve. Equation (1) is shown in Fig. 2, in each case with T_1 chosen so that the midpoint of the experimentally observed transition coincides with that for the equation. In most cases, the slope of the experimental points for the central portion of the transition is in fair agreement with that predicted by Eq. (1). In Fig. 3 are shown the critical-field-versus-temperature points derived from all such determinations. The plotted temperature is that at the midpoint of the transition. From elementary magnetostatics the corresponding critical field, i.e., the equatorial field, is $5H/4$. The critical-field data of Fig. 3 serve to determine the transition temperatures as the intercepts of the critical-field curves on the temperature axis. The average slopes corresponding to the data appear somewhat smaller than for pure Sn. The dependence of T_c on laminar spacing is discussed in a later section.

In order to observe isothermal transitions, extensive measurements were made at 3.277°K on all samples in both increasing and decreasing field. The results are shown in Fig. 4. The approximately triangular shape of these isotherms in increasing field is consistent with the behavior expected of a type-I superconductor. In general the magnetization curve of an ellipsoidal sample should have an initial susceptibility given by

$$M/H = -(1/4\pi)/(1-\alpha), \quad (3)$$

where α is the demagnetizing coefficient. The peak of the curve, where field penetration first occurs, should be located at a field H_{c1} such that

$$H_{c1} = H_c(1-\alpha). \quad (4)$$

The observed α for each sample is recorded in Table I, and may be compared with that for a sphere, 0.333. The diamagnetic susceptibility, i.e., the slope of the initial

TABLE I. Sample properties.^a

Ingot growth rate (cm/h)	Laminar period $\times 10^4$ (cm)	$10^4 d_s$ (cm)	$10^4 d_n$ (cm)	T_c ($^{\circ}\text{K}$)	$H_c(3.277)$ (Oe)	α
...	Sn	3.722	61	0.320
0.3	7.5	6.8	0.66	3.716	58	0.344
0.3	6.2	5.6	0.54	3.706	55	0.332
0.5	3.9	3.6	0.34	3.699	55	0.283
3.4	2.0	1.8	0.18	3.680	53	0.308
8.8	0.8	0.7	0.07	3.668	52	0.300

^a Definition of symbols: d_s , width of Sn-rich layer; d_n , width of Zn-rich layer, T_c , transition temperature; $H_c(3.277)$, critical field at 3.277°K ; α , demagnetizing coefficient, determined from 3.277°K isotherm.

leg, is seen to fall somewhat below that expected, the discrepancy being generally greater for the larger laminar spacings. The samples exhibit varying degrees of trapped flux. There is apparently very little "supercooling," however, as the critical field determined in increasing field is close to that in decreasing field.

The transition temperatures determined from Fig. 2 and the critical fields determined from Fig. 4 are tabulated in Table I. H_c shows the proper qualitative variation with T_c . This may be seen more fully in Fig. 5, which shows critical-field data for the 2- μ sample over the temperature range 3.0–3.7°K. Critical fields at the lowest three temperatures were determined from isotherms, while the points near T_c are taken from the constant-field transitions of Fig. 2. Also shown are calculated critical-field curves based on the transition temperatures for the 2- μ sample and for pure Sn. The calculated curves were obtained from the expression⁹

$$H_c/H_0 = 1 - 1.078(T/T_c)^2 - 0.103(T/T_c)^3 + 0.181(T/T_c)^4, \quad (5)$$

where $H_0 = 81T_c$. The 2- μ data are seen to agree fairly well with Eq. (5) over the region of measurement, although the constant-field determinations near T_c appear to give somewhat smaller H_c . It is interesting to note, in light of the introductory discussion, that the critical-field behavior shown in Fig. 5 for the 2- μ spacing

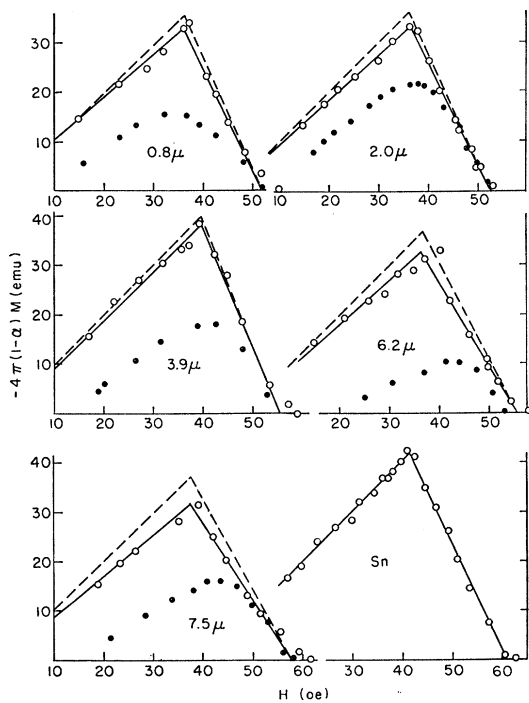


FIG. 4. Magnetic isotherms at 3.277°K. Magnetic moment per unit volume versus applied magnetic field H . Solid curves show approximate relations corresponding to data, while dashed lines are the theoretical isotherms corresponding to α . α is the demagnetizing coefficient determined from the observed ratio of H at the apex of the solid curve to H at the $M=0$ intercept.

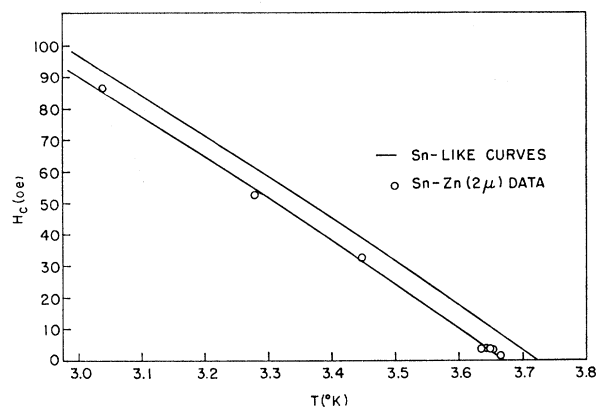


FIG. 5. Critical-field curve for 2- μ laminar spacing. Critical-field data for one sample determined by isotherm measurements at several temperatures. Solid curves are critical-field curves for Sn calculated from expression appearing in literature, using $T_c = 3.66^\circ\text{K}$ and $T_c = 3.72^\circ\text{K}$.

is quite different from what would be expected if, in the superconducting state, an appreciable magnetic field existed in the Zn-rich layers. In the latter case, an increase of critical field over that for the bulk material would be expected due to size effects, since the penetration depth in the impure Sn layers should become comparable to the 2- μ layer thickness near T_c .¹⁰ No such distortion of H_c is evident in Fig. 5. This is consistent with the expectation that the eutectic structure behaves like a continuous superconducting material, the penetration depth at the surface of the sphere being small in comparison with the sphere diameter. The results illustrated by Figs. 2, 4, and 5, therefore, suggest that these eutectic samples may be described approximately as type-I superconductors having flux-trapping centers.

Dependence of T_c on Laminar Spacing

The critical-field measurements near T_c and at 3.277°K show that the transition temperatures of the eutectics are displaced relative to each other in correspondence with the laminar spacing in the sample, the total spread of T_c being about 0.05°K. Since the smaller spacings have the lower T_c , the dependence is qualitatively that expected for proximity effects. In order to discuss further this variation of transition temperature with laminar spacing we first of all summarize the results of existing theory. The theory of proximity effects in superimposed films has been developed most extensively by De Gennes¹¹ and by Werthamer,¹² with their colleagues. Generally speaking, the useful relations apply to the case of a single layer of normal metal, of thickness d_n , in contact with a single layer of super-

¹⁰ E. A. Lynton, *Superconductivity* (John Wiley & Sons, Inc., New York, 1962). A review of this effect is given in Chap. VII.

¹¹ P. G. De Gennes and E. Guyon, *Phys. Letters* **3**, 168 (1963); P. G. De Gennes and D. Saint James, *ibid.* **4**, 151 (1963). P. G. De Gennes, *Rev. Mod. Phys.* **36**, 225 (1964).

¹² N. R. Werthamer, *Phys. Rev.* **132**, 2440 (1963); see also Ref. 2.

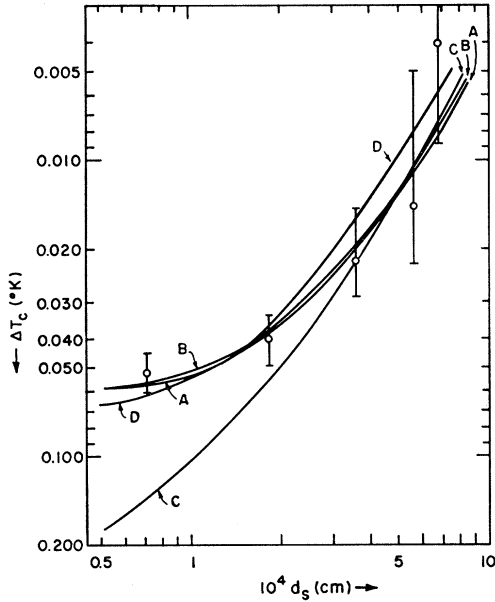


FIG. 6. Dependence of transition temperature on laminar spacing. The quantity ΔT_c is defined as $T_{cs} - T_c$ where T_c is the observed transition temperature and T_{cs} is assumed to be 3.720°K. The abscissa gives the width of the Sn-rich layers. Symbols labeling the theoretical curves refer to parameters of the theory listed in Table II.

conducting metal, of thickness d_s . An implicit relation for the transition temperature of such a double layer is given as follows¹²:

$$(t^{-1}-1)^{1/2} \tan[k_s(t)d_s] = (\theta^{-1}-1)^{1/2} \tan[k_s(\theta)d_s] \times [\xi_n(t)k_n(t)/\xi_n(\theta)k_n(\theta)] \tanh(k_n d_n), \quad (6)$$

where $t = T_c/T_{cs}$ is the ratio of the transition temperature of the sandwich to that of the superconducting material in bulk, d_s is the thickness of the superconducting layer, d_n is the thickness of the normal layer, $\xi_n(t) = \hbar(v_f l)_n / (6\pi k_b T_c)$ is the coherence length of normal material having Fermi velocity v_f and mean free path l (k_b is the Boltzmann constant),

$$k_s(t) = (2/\pi \xi_{ss})(1-t)^{1/2}, \\ k_n(t) = (1/\xi_{ns}) \{1 - (T_{cn}/T_c)^{4/\pi^2}\}^{1/2}$$

(in which T_{cn} is the transition temperature of the normal material in bulk),

$$\xi_{ss} = \hbar(v_f l)_s / (6\pi k_b T_{cs}), \\ \theta = \lim_{d_n \rightarrow \infty} (T_c/T_{cs}).$$

An implicit relation is also given for θ , as follows¹²:

$$N_s \xi_{ss} (2/\pi) (\theta^{-1}-1)^{1/2} \tan[k_s(\theta)d_s] = N_n \xi_{ns} \xi_n(\theta) k_n(\theta), \quad (7)$$

where

$$\xi_{ns} = (\hbar(v_f l)_n / 6\pi k_b T_{cs}).$$

N_s and N_n designate the density of states at the Fermi level per unit energy interval and unit volume, for the

superconducting and normal material, respectively. We denote by ΔT_c the difference $T_{cs} - T_c$, that is, the depression of the transition temperature of the combined material below that of the superconducting component when by itself. Solution of Eqs. (6) and (7) yields ΔT_c as a function of d_n and d_s , provided we know T_{cn} , T_{cs} , $(v_f l)_n$, $(v_f l)_s$, and N_s/N_n . As pointed out by Werthamer *et al.*,¹² the product $v_f l$ is best calculated by use of the conductivity σ and the electronic-specific-heat coefficient per unit volume, γ , through the expression:

$$v_f l = (\pi k_b / e)^2 (\sigma / \gamma). \quad (8)$$

T_{cs} is usually known, while T_{cn} is either known or left as an adjustable parameter to be determined from the experimental results. N_s/N_n may be equated to the ratio (γ_s/γ_n) .¹³

We now wish to extend the above expressions to the case of a periodic structure. Denoting by ΔT_c the change in transition temperature for the double-layer case and by $(\Delta T_c)'$ that for the periodic structure, we wish to show that

$$(\Delta T_c)'(d_n, d_s) = \Delta T_c(d_n/2, d_s/2). \quad (9)$$

The argument is as follows: Equations (6) and (7) result from the solution of a differential equation in which the dependent variable is the energy-gap function Δ and the independent variable is the position vector \mathbf{r} .^{11,12} The film thickness in the double-layer geometry enters by way of the following boundary condition:

$$[d\Delta(\mathbf{r})/dx]_{x=d_s} = [d\Delta(\mathbf{r})/dx]_{x=-d_n} = 0. \quad (10)$$

This condition requires zero slope of the gap function at the two metal-vacuum interfaces. When we go over to the periodic structure, symmetry considerations require that the slope be zero at the center of each layer, i.e.,

$$[d\Delta(\mathbf{r})/dx]_{x=d_s/2} = [d\Delta(\mathbf{r})/dx]_{x=-d_n/2} = 0. \quad (11)$$

The boundary condition at the superconducting-normal interface (i.e., at $x=0$) has not changed. The required solution for the periodic structure must therefore be that derived by substituting $d_n/2$ and $d_s/2$ into the double-layer solution.

In order to compare the theory with our experimental results we have combined Eqs. (6) and (7), and have substituted $d_s/2$ and $d_n/2$ in accordance with the preceding argument. This gives the following relation:

$$(t^{-1}-1)^{1/2} \tan[k_s(t)d_s/2] = (\pi/2)(N_n/N_s)(\xi_{ns}/\xi_{ss}) \times \{1 - (T_{cn}/T_c)^{4/\pi^2}\}^{1/2} \tanh[k_n d_n/2]. \quad (12)$$

It is instructive to consider the form taken by Eq. (12) in the limit of small d_s , d_n ($k_n d_n/2 \ll 1$, $k_s d_s/2 \ll 1$). Using previous definitions of the quantities involved, the following approximate relation is derived:

$$(t^{-1}-1)^{1/2} (1-t)^{1/2} \cong (\pi/2)^2 (N_n/N_s) \times \{1 - (T_{cn}/T_c)^{4/\pi^2}\} (d_n/d_s). \quad (13)$$

¹³ A. H. Wilson, *The Theory of Metals* (Cambridge University Press, Cambridge, England, 1953), 2nd ed., Chap. VI, p. 144.

TABLE II. Parameters for ΔT_c curves.^a

Curve designation	T_{cs} (°K)	T_{cn} (°K)	γ_s (ergs/cm ³ °K)	γ_n (ergs/cm ³ °K)	ρ_s	ρ_n
A	3.720	2.7	1.1	0.6	0.12	1
B	3.720	2.7	1.1	0.6	0.14	0
C	3.720	0.9	1.1	0.6	0.14	2
D	3.720	2.5	1.1	0.6	0.14	2

^a Definition of symbols: T_{cs} , T_{cn} , assumed bulk transition temperatures of Sn-rich and Zn-rich phases, respectively; γ_s , γ_n , electronic-specific-heat coefficients for pure Sn and Zn, taken from *American Institute of Physics Handbook* (McGraw-Hill Book Company, Inc., New York, 1957); ρ_s and ρ_n , assumed ratio of electrical resistivity at 4°K to that at room temperature, for Sn-rich and Zn-rich layers.

According to Eq. (13) the transition temperature in the limit of small d_s , d_n depends only on N_n/N_s , T_{cn} , T_{cs} , and the ratio d_n/d_s . Since, for the eutectic structure, d_n/d_s is independent of laminar spacing, we see that with decreasing laminar period T_c should approach a constant value determined by the specific-heat ratio and the bulk transition temperatures of the two metals. Conversely the limiting experimental T_c could serve to determine an otherwise unknown T_{cn} or N_n/N_s .

In Fig. 6 we have compared our experimental results for T_c with the predictions of Eq. (12), using parameters listed in Table II. Regarding the choice of parameters for the theoretical curves, γ_s and γ_n are assumed to be close to the pure-metal values, since the Zn-rich phase is believed to contain only about 0.1 at.% Sn,⁶ and since γ for Sn does not change markedly with addition of impurities.¹⁴ The choice of T_{cs} is imposed by the data of Fig. 3, which shows that the apparent limiting transition temperature at large spacing is also close to that of pure Sn, i.e., 3.72°K. The resistivities of the two phases and the transition temperature of the Zn-rich phase have been varied to give the three theoretical curves. It may be seen from Fig. 6 that ρ_s is determined mainly by the large-spacing data, while T_{cn} is determined mainly at small spacings. The last conclusion is consistent with the previous discussion concerning the limiting T_c at small laminar spacing. Regarding the numerical values of the quantities, ρ_s is expected to be related to the concentration and impurity resistivity of Zn dissolved in the Sn-rich phase, through the expression

$$\rho_s = \rho_s' c_s, \quad (14)$$

where ρ_s' is the increase in the residual resistance ratio of Sn due to addition of unit concentration of Zn, and c_s is the Zn concentration in the Sn-rich phase. ρ_s' measured for Sn(Zn) solid solutions lies between 0.015 and 0.050 per atomic percent.¹⁴ Using $\rho_s = 0.12$ the implied concentration range is thus 2–8 at.% Zn. This may be compared with reported values for the Zn solubility varying from 0 to 7 at.% and with the suggested value of 2 at.%.⁶ ρ_s is therefore in fair agreement with its expected magnitude. The appraisal of T_{cs} is a little less certain. It is known that the addition of Zn in

amounts of less than 1 at.% results in a lowering of the Sn transition temperature.¹⁴ The transition temperature at higher Zn concentrations has apparently not been investigated. For some impurities, however, continued increase of concentration results in an eventual raising of the transition temperature back to its value for pure Sn, and even above.¹⁴ If this is true of Zn impurities, the indicated concentration of several at.% may correspond to a T_{cs} close to that of pure Sn, as observed.

ρ_n is not derivable from the experimental results, since, as apparent from Fig. 6, values can be assigned over its physically plausible range without appreciable change in the theoretical curves. This fact probably is related to the condition, applicable to our samples, that $k_n d_n/2 \leq 1$ or $\tanh(k_n d_n/2) \cong k_n d_n/2$. Under this condition the coherence length ξ_{ns} cancels out in the right side of Eq. (12) and thus ρ_n is not critical.

The small spacing data show smaller ΔT_c than expected from the assumption that T_{cn} is 0.9°K, the accepted transition temperature of Zn. The required T_{cn} is instead about 2.7°K. The origin of this discrepancy is not clear. The question of the T_{cn} dependence has been of some importance in thin film work² because of attempts to deduce the unknown T_{cn} of the normal metal components. There is, however, a lack of experimental tests of the theory using normal metals of known T_{cn} . The most relevant thin film test of the theoretical T_{cn} dependence is that of Hauser and Theurer² on Pb-Al films. Their results, obtained with d_n/d_s ratios much larger than that of our experiments, were consistent with the accepted transition temperature of Al.

A possible circumstance which could lead to the small spacing discrepancy would be differential strain in the two phases due to cooling. Such strain in the Zn layers could conceivably lead to an anomalous T_{cn} . It is known that the transition temperature of a superconductor is highly dependent on the density of states at the Fermi level,¹⁵ and that the properties of the Zn Fermi surface are sensitive to pressure.¹⁶ Studies of the effect of pressure on transition temperature in Zn, however, are lacking. Another possible explanation of the results would be a dependence of composition on laminar spacing. Calculations indicate, however, that the two-week anneal at 140°C should be sufficient to equilibrate the samples at the Zn solubility corresponding to that temperature, and that further changes at room temperature should be small.

SUMMARY

An investigation was made of the superconductivity of Sn-Zn eutectic alloys having the characteristic two-phase laminar structure. The magnetic transitions were found to approximate those of a type-I superconductor with respect to the shape of the transitions and the form of the critical field-versus-temperature relationship.

¹⁵ Reference 10, p. 122.

¹⁶ W. A. Harrison, Phys. Rev. **118**, 1190 (1960).

¹⁴ E. A. Lynton, B. Serin, and M. Zucker, J. Phys. Chem. Solids **3**, 165 (1957).

Special emphasis was given the dependence of transition temperature on laminar period. The dependence was found to be in qualitative, but not quantitative, agreement with proximity-effect theory developed for superimposed films.

ACKNOWLEDGMENTS

The authors wish to thank J. L. Schmit, Dr. J. A. Sartell, and Dr. R. A. Swalin for consulting on various aspects of the investigation, and Dr. M. D. Blue for comments concerning the manuscript.

Diffusion Constants near the Critical Point for Time-Dependent Ising Models. I*

KYOZI KAWASAKI

Department of Chemistry, Massachusetts Institute of Technology, Cambridge, Massachusetts

(Received 18 November 1965)

The diffusion constant of spins in ferromagnets or of molecules in binary mixtures near the critical point is discussed employing a time-dependent Ising model in which spin interactions are replaced by certain temperature-dependent transition probabilities of spin exchange. The spin diffusion constant is calculated with the single approximation of replacing a reduced spin distribution function by its value for local equilibrium with a given inhomogeneous spin density. The behavior of the diffusion constant near the critical point is dominated by a factor χ^{-1} , where χ is the magnetic susceptibility. This problem is also studied with the use of the Bethe lattice. The effects of surrounding spins on the transition probability for spin exchange are found to be essential for obtaining the critical slowing-down near the critical point. In view of this, Kociński's calculation of the spin diffusion constant is critically discussed.

1. INTRODUCTION

THE behavior of various transport coefficients near the critical point is one of the most interesting but least understood problems in statistical physics today, and a large body of experimental work is appearing without proper theoretical understanding.¹ Among these phenomena, the problem of spin diffusion in ferromagnets near the Curie point has received more theoretical treatment than others because of the apparent simplicity of the problem.²⁻⁷ In the present paper we shall also be concerned with this problem. This problem can be translated into the problem of molecular diffusion in binary mixtures if we ignore the quantum nature of the Heisenberg system.⁸ The spin density and the external magnetic field correspond to the concentration and the chemical potential, re-

spectively. In this paper we shall use the terminology of the spin system.

We shall now briefly discuss the present status of this problem. The most common theoretical argument goes somewhat like this.^{2,4,9} Let us consider an isolated spin system and divide it into small but macroscopic cells. Let the fluctuation of the magnetization of the j th cell be M_j . Then the excess entropy associated with this fluctuation is written as

$$\Delta S = -k_B/2 \sum_{jl} a_{jl} M_j M_l \quad (1.1)$$

$$= -k_B/2n \sum_q \lambda_q M_q M_q^* \quad (1.2)$$

where n is the total number of cells and k_B the Boltzmann constant, and we have introduced the following Fourier transforms:

$$\lambda_q \equiv \sum_l a_{jl} \exp[i\mathbf{q} \cdot (\mathbf{r}_j - \mathbf{r}_l)], \quad (1.3)$$

$$M_q \equiv \sum_l M_l \exp(-i\mathbf{q} \cdot \mathbf{r}_l), \quad (1.4)$$

where \mathbf{r}_j denotes the position vector of the j th cell. Since the probability of occurrence of the fluctuation M_q is proportional to $\exp(\Delta S/k_B)$, we have

$$\lambda_q^{-1} = n^{-1} \langle M_q M_q^* \rangle = k_B T \chi_q, \quad (1.5)$$

where χ_q is the wave-vector-dependent magnetic susceptibility and T the temperature. Thermodynamics of irreversible processes then gives the relaxation rate

* A portion of this work was supported by the National Science Foundation.

¹ Proceedings of Critical Phenomena Conference, Washington, D. C., 1965 (to be published.)

² L. Van Hove, Phys. Rev. **95**, 249 (1954); **95**, 1374 (1954); P. G. de Gennes, Comm. Energie At. (France) Rappt. No. 925, 1959; (unpublished); P. G. de Gennes and J. Villain, J. Phys. Chem. Solids **13**, 10 (1960); P. G. de Gennes, in *Magnetism*, edited by G. T. Rado and H. Suhl (Academic Press Inc., New York, 1963), Vol. III.

³ H. Mori and K. Kawasaki, Progr. Theoret. Phys. (Kyoto) **27**, 529 (1962).

⁴ H. Mori, Progr. Theoret. Phys. (Kyoto) **30**, 576 (1963).

⁵ H. S. Bennett and P. C. Martin, Phys. Rev. **138**, A608 (1965).

⁶ J. Kociński, Acta Phys. Polon. **24**, 273 (1963).

⁷ H. Mori, Progr. Theoret. Phys. (Kyoto) **34**, 399 (1965).

⁸ T. L. Hill, *Statistical Mechanics* (McGraw-Hill Book Company, Inc., New York, 1956).

⁹ P. Debye, Phys. Rev. Letters **14**, 783 (1965).

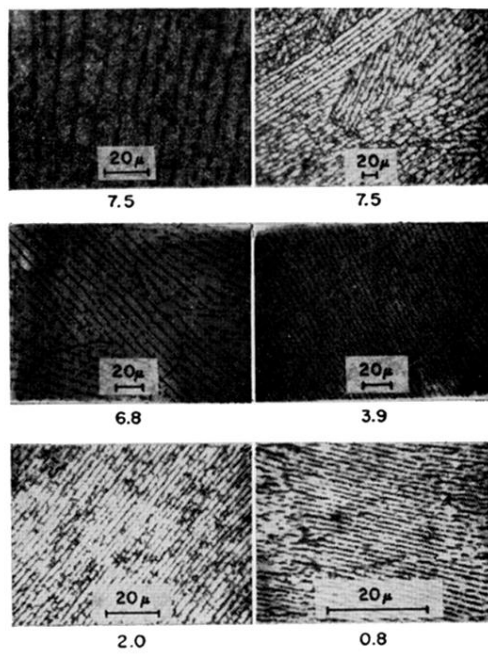


FIG. 1. Photomicrographs of laminar structure. Surfaces are planes lying perpendicular to direction of temperature gradient in the various ingots. Ingots are identified by period in microns given below each photograph. Scale is given by length of 20- μ symbol on photograph. Eutectic domains may best be seen in photomicrograph on upper right.